Influence of the Orbital Configuration of a Four-rail Electromagnetic Launcher on Joule heat

Pengxiang Zhang, Tao Shu

Air Defense and Missile Defense College, Air Force Engineering University, Xi'an 710051, China

Corresponding author: Pengxiang Zhang (e-mail: qianxing979@163.com).

ABSTRACT During the working process of electromagnetic launcher, the rapid temperature rise caused by heat accumulation has an important influence on the performance and life of the armature and rail. In order to better solve the thermal ablation problem of the armature and rail of the four-rail electromagnetic launcher, three different configurations of the rail and armature model are established, using the finite element method, the Joule heating characteristics of the three structures are simulated, analyzed and compared. The simulation results show that the Joule heat of the armatures of the three structures is concentrated at the throat, and the Joule heat of the rail is concentrated at the edge of the rail and the contact surface of the pivot rail; among the three structures, the electromagnetic launcher of the convex rail-concave armature structure has the smallest temperature rise rate, in addition, the peak temperature on the contact surface between the armature and the guide rail is the lowest, the safety of the ammunition is the highest, and the performance is more advantageous than the electromagnetic launcher of the other two structures.

INDEX TERMS Electromagnetic launch technology; Finite element simulation; Orbital configuration; Quadrupole magnetic field; Temperature characteristics.

I. INTRODUCTION

ELECTROMAGNETIC launch refers to a new type of launch method that uses the interaction between current and magnetic field to generate a strong electromagnetic thrust to achieve the purpose of acceleration. Through precise control of pulse power output, electromagnetic launch can achieve highly controllable launch thrust and real-time response, effectively ensuring launch stability. With the deepening of research, the electromagnetic launcher has developed from the original double-rail launch to the four-rail launcher [1-3]. Compared with the ordinary double-rail launcher, the four-rail launcher is not only more stable in structure, but also has greater launch efficiency. At present, one of the main reasons affecting the development of four-rail electromagnetic launcher is the life span problem, and an important factor affecting the life span of electromagnetic launcher is the ablation of the rail and armature. The thermal effect caused by the instantaneous high current passed into the electromagnetic launcher during its operation can cause damage to the armature and the rail. Due to the demand of the launch, the current size is often difficult to change, thus it is necessary to improve the heat concentration problem caused by the current concentration by changing the structural parameters of the armature and the rail, thus reducing the degree of thermal damage to the armature and the rail and extending the service life of the electromagnetic launcher.

The structure of the armature and orbit of the electromagnetic launcher and the Joule thermal effect have been studied extensively by domestic and foreign scholars. Tengda Li et al. investigated four-rail electromagnetic launchers with different armature-rail configurations and derived their current distribution and hydrostatic properties [4-5]; Barber et al. explored the solid armature ablation turning mechanism and pointed out that the turning process is mainly affected by the Joule heat of the current [6-7]; Motes D learned from simulations in Maxwell and E-Physics that the Joule heat caused by the current is the main reason for the temperature rise of the launcher [8]. Lingkang Zhao established the heat conduction equation containing the internal heat source and applied the Green's function to find the theoretical solution of the armature and orbital temperature fields, and explored the effect of non-Fourier effect on the temperature distribution [9]; Xiaojiang Li et al. mainly conducted numerical simulations on the temperature and thermal stress during the launch of electromagnetic launchers with various armature and orbital configurations, and concluded that the convex rail has better characteristics in terms of temperature rise [10]. From the current research results, the study of the thermal characteristics of electromagnetic launcher only stays at the stage of two-rail model, while the study of the effect of the structure of four-rail electromagnetic launcher on the thermal characteristics is rare. Based on the above analysis, the authors simulate the

Joule heat characteristics of four-rail electromagnetic launcher with three different armature structures, so as to investigate the temperature distribution law caused by Joule heat, and analyze the Joule heat of electromagnetic launcher with different armature structure parameters, in order to seek the influence law of armature structure changes on Joule heat concentration, and provide some reference for the structural design of transmitting devices.

II. MODEL AND SIMULATION CONDITIONS

A. Geometric model

The four-rail electromagnetic launcher model used in this paper is shown in Fig. 1. The four rails are distributed in a uniform circular array with the armature as the center, and the trapezoidal pulse current flows in from the two opposite rails, flows through the armature, and then flows out from the remaining two rails. The current in the armature is orthogonal to the magnetic field generated by the current flowing in the rails, which generates electromagnetic thrust and propels the armature to accelerate its motion. Due to the symmetrical distribution of the four rails and the symmetry of the armature structure, the magnetic fields generated by the currents in the region at the center of the armature cancel each other, resulting in an electromagnetic shielded region. Taking into account the current flow on the armature and the practicality of carrying ammunition on the armature, the hollow design of the armature as shown in the Fig. 2 provides a good electromagnetic shielding environment for the ammunition carried in it, while reducing the mass of the armature and improving the emission efficiency of the electromagnetic launcher. The large contact surface on the armature arm can effectively ensure the effective contact between the armature and the rail, and the deflecting arc structure at the throat of the armature can reduce the concentration problem of current.

To study the relationship between thermal damage of the pivot rail and the pivot rail structure of the four-rail electromagnetic launcher, two electromagnetic launchers with different pivot rail structures, convex rail (concave armature) and concave rail (convex armature), were designed on the basis of the planar-rail electromagnetic launcher. The four-rail electromagnetic launcher model with three pivot rail configurations is shown in Fig. 3.

Among them, the material design of armature and rail [11] is shown in Table I. The parameters of the electromagnetic launcher model are shown in Table II.

B. Simulation conditions

The electromagnetic force required for the instantaneous electromagnetic emission usually requires a strong pulsed power supply, and the strong current generated by the direct use of the pulsed power supply will lead to a large oscillation of the electromagnetic force generated on the electromagnetic launcher, and the energy conversion rate is not high, in order to avoid this situation, the trapezoidal

current excitation is usually used. In the simulation process of this paper, the trapezoidal current excitation is applied to the rail as shown in Fig. 4, and the application method is shown in Fig. 1. The current rising edge phase is 0-0.02ms, the constant current phase is 0.02-5ms, and the constant current phase current is 300KA.
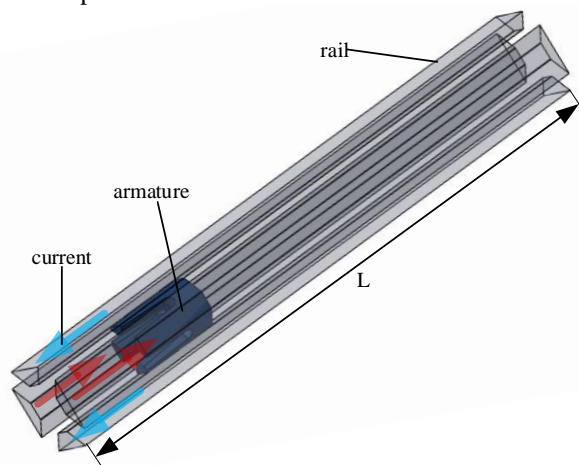

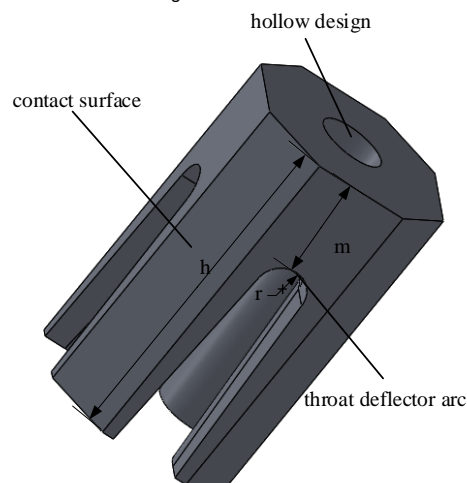**FIGURE 1.** Four-rail electromagnetic launcher model
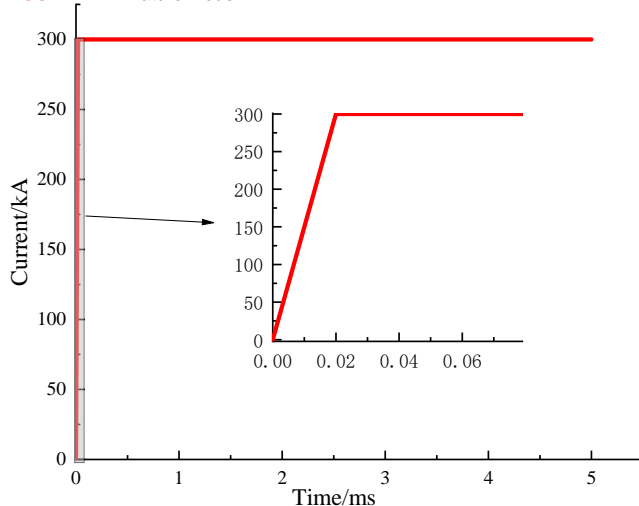

FIGURE 2. Armature model

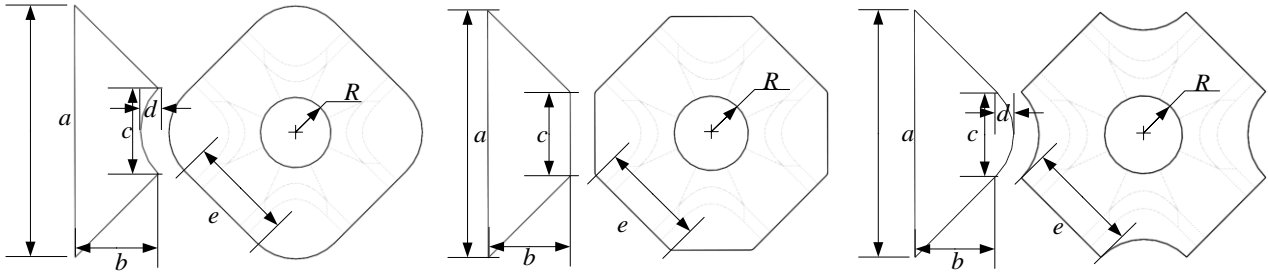**FIGURE 4.** Current model

FIGURE 3. Rail-armature model with different configurations

TABLE I. Electromagnetic launcher material parameters

	Materials	Density / $(kg \times m^{-3})$	Conductivity / $(S \times m^{-1})$	Specific Heat Capacity / $J/(kg \cdot K)$
Rail	copper	8.66×10^{3}	5.80×10^{7}	385
Armature	aluminum	2.70×10^{3}	3.76×10^{7}	900

TABLE II. Electromagnetic launcher model parameters

Parameters	a	b	c	d	e	m	h	R	r
Value/mm	26	8.6	8.8	1.83	11.52	12.00	40.00	4.00	3.00

III. Theoretical analysis

During the operation of the four-rail electromagnetic launcher, current flows in from the rail, flows through the armature and then out from the rail, and due to the existence of resistance, a significant portion of the electrical energy is dissipated in the form of heat during transmission. The resistance of the electromagnetic launcher can be expressed as:

$$R = R_a + R_r + R_{con} \tag{1}$$

Where, R_a denotes the resistance of the armature, R_r denotes the resistance of the rail, and R_{con} denotes the resistance of the contact surface between the armature and the rail. From the microscopic point of view, during the operation of the electromagnetic launcher, not all the contacts between the armature and the rail are ideal, Holm pointed out in his research that the contact surfaces of different objects form a current circuit through "a-spot"[12], so the contact between the armature and the rail can be shown in Fig. 5.
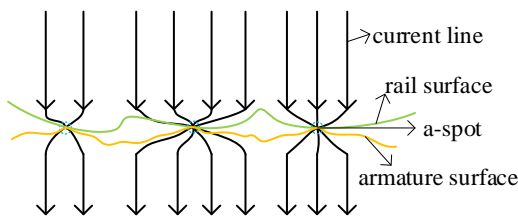

FIGURE 5. Schematic diagram of pivot rail contact surface

As shown in the Fig. 5, when the current flows through the contact surface of the pivot rail, the current line will contract to the a spot, thus causing the circuit resistance to increase, the part of the contact resistance is called the contraction resistance R_s; in addition, there will be a film layer formed by oxides, etc., on the surface of the object, resulting in an increase in the circuit resistance, which is also part of the contact resistance, called the film resistance R_m, therefore, the contact resistance can be expressed as:

$$R_{con} = R_s + R_m \tag{2}$$

Usually, when the armature and the rail are assembled, the film layer resistance is destroyed. To simplify the analysis, the contraction resistance is regarded as the full contact resistance between the rail and the armature, and according to Holm's study, the contact resistance of a single a spot under general energization can be expressed as:

$$R_s = \frac{\rho_a + \rho_r}{4r} \tag{3}$$

where ρ_a and ρ_r denote the conductivity of the two contacting objects, i.e., the armature and the rail, respectively, and r denotes the radius of a single circular a-spot. However, the overall shrinkage resistance is affected by the number and size of a-spots, but also by the shape and size of the cluster of spots, but when the a-spots are small, the effect of the cluster of spots can be neglected. Assuming that there are n circular a-spots in the contact section between the rail and the armature, according to Fig. 5, the n a-spots can be regarded as parallel, and the expression of shrinkage resistance is:

$$R_s = \frac{\rho_a + \rho_r}{4nr} \tag{4}$$

and the conductive contact area formed by n a-spots can be expressed as:

$$S = n\pi r^2 \tag{5}$$

In turn, the conductive contact area can be characterized by the contact pressure F_p, metal hardness H, i.e.

$$S = \eta \frac{F_p}{H} \tag{6}$$

where η is the correction factor for the conductive contact area and the nominal contact area, which is usually considered to be much less than 0.1, and is the hardness of

the softer material in the contact object, taken as the hardness of the armature. The number of spots can be estimated by: 10 on the nominal contact surface/ $4mm^2$. Combining equations (2) to (6), the contact resistance expression can be obtained as follows

$$R_{con} = \frac{\rho_a + \rho_r}{4}(\frac{\pi H}{n\eta F_p})^{\frac{1}{2}} \quad (7)$$

Thus, the Joule heat Q_{con} at the contact surfaces of the four pivot rails of the four-rail electromagnetic launcher can be expressed as

$$Q_{con} = 4\int_0^T I^2 R_{con} dt = \int_0^T I^2 (\rho_a + \rho_r)(\frac{\pi H}{n\eta F_p})^{\frac{1}{2}} dt \quad (8)$$

And the Joule heat generated by the armature and the orbit is:

$$Q_a = \int_0^T I^2 R_a dt \quad (9)$$

$$Q_r = \int_0^T I^2 R_r dt \quad (10)$$

where I denotes the incoming current and T the time of operation of the electromagnetic launcher. According to the expression, it can be seen that Joule heat is cumulative in time and closely related to the distribution of current density in space [13].

IV. Simulation analysis

A. Joule heat analysis of different configurations of electromagnetic launchers

Using ANSYS and Maxwell software to conduct electromagnetic-temperature coupling analysis, import the electromagnetic field calculation results in Maxwell into the transient thermal component of ANSYS. In order to better simulate the actual working state of the electromagnetic launcher, the surface of the electromagnetic launcher is set to be air natural convection, and the convection heat transfer coefficient is $3W/mm^2 \cdot ℃$. The temperature distribution of the electromagnetic launcher caused by Joule heating under different pivot-rail configurations is obtained. Fig. 6 is a schematic diagram of the highest temperature change caused by Joule heating of the four-rail electromagnetic launcher with three structures

Let the average temperature rise rate of the electromagnetic launcher be:

$$k = \frac{T_{max} - T_{min}}{t} \quad (11)$$

Where T_{max} represents the maximum temperature rise during the operation of the electromagnetic launcher, T_{min} represents the initial temperature at the beginning of the operation of the electromagnetic launcher, and t represents the operating time. According to this equation, the average temperature rise rate of the planar rail-planar armature electromagnetic launcher is $54.47℃/ms$, the average
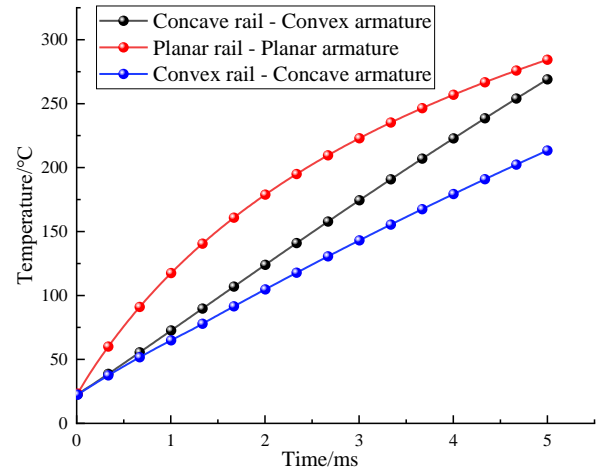

FIGURE 6. Schematic diagram of the maximum temperature variation of electromagnetic launchers of different structures

temperature rise rate of the concave rail-convex armature electromagnetic launcher is $49.40℃/ms$, the average temperature rise rate of the convex rail-concave armature electromagnetic launcher is $40.38℃/ms$, and the average temperature rise rate of the convex rail-concave armature electromagnetic launcher is the lowest, which is 25.87% lower than the average temperature rise rate of the planar rail-planar armature electromagnetic launcher and 18.26% lower than the average temperature rise rate of the concave rail-convex armature electromagnetic launcher. The average temperature rise rate is 18.26% lower than that of the concave rail-convex armature structure. Therefore, the convex rail-concave armature structure is more beneficial to mitigate the temperature rise problem of the electromagnetic launcher and thus prolong the life of the electromagnetic launcher.

To further study the temperature distribution of each part on the electromagnetic launcher, the temperature field analysis was performed on the armature and the rail, respectively.

Fig. 7 shows the temperature distribution due to Joule heat at the armature of the four-rail electromagnetic launcher for the three configurations, and the units in the figure are degrees Celsius (°C).

As shown in the Fig. 7, the peak temperature of the armature part during the operation of the electromagnetic launcher of the concave rail-convex armature structure is 269.03°C, that of the planar rail-plane armature structure is 284.36°C, and that of the convex rail-concave armature structure is 223.88°C. The peak temperature during operation of the electromagnetic launcher with the convex rail-concave armature structure was the smallest, 60.48°C smaller than that of the planar rail-planar armature structure and 45.15°C smaller than that of the electromagnetic launcher with the concave rail-convex armature structure. Compared with the other two structures, the convex rail-concave armature structure electromagnetic launcher has a greater advantage in mitigating the Joule heat temperature rise in the armature area.
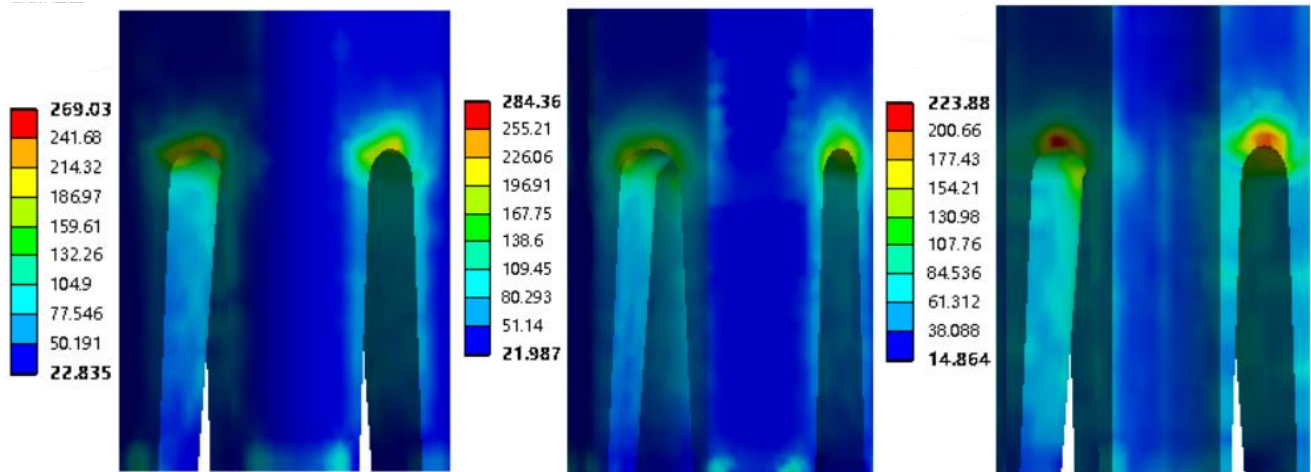
FIGURE 7. Schematic diagram of armature temperature distribution of different configurations
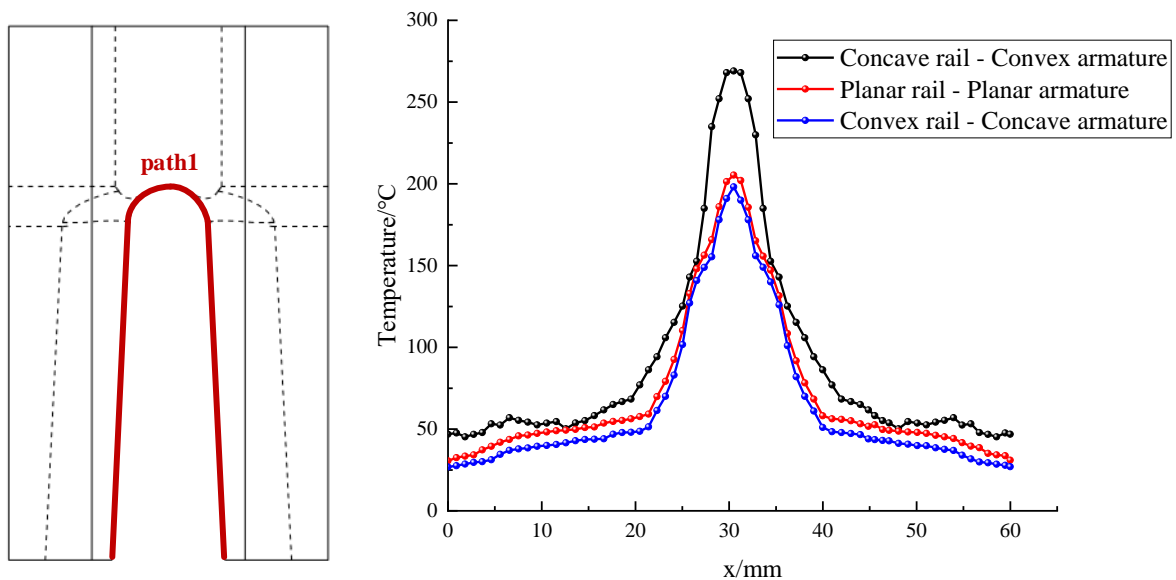

FIGURE 8. Schematic diagram of path 1 and temperature distribution

In addition, all three configurations of the electromagnetic launcher exhibit Joule heat concentration, with the most pronounced location in the throat inflow arc region. The concave-rail-convex armature structure and the planar-rail-plane armature structure have a more obvious Joule heat concentration problem at the end of the armature arm, while the convex-rail-concave armature structure has a more uniform temperature distribution on the contact surface of the armature rail [14].

The armature throat, where the Joule heat concentration problem is obvious, is selected for the study, and the distribution of Joule heat-induced temperature at the throat is analyzed. Fig. 8 shows the temperature distribution of the throat path of different armature structures. As shown in Fig. 8, the temperature distribution at the throat of the armature for all three structures of the electromagnetic launcher shows an axisymmetric pattern, and the peak temperature occurs at

the center of the armature throat, and the temperature decreases from the center of the armature to the end of the armature. The fastest temperature drop is located at the junction of the armature throat and armature arm, which also indicates that the Joule heat of the armature is concentrated at the throat of the armature. Also, it can be seen from the figure that the temperature of the electromagnetic launcher of the convex rail-concave armature structure is less than that of the other two structures at any point along the selected throat path.

To investigate the influence of the electromagnetic launcher pivot rail configuration on the armature carrying capacity under the temperature field angle, the temperature of the path at the edge of the electromagnetic shield hole shown in Fig. 9 was analyzed and the temperature distribution on the path was obtained as shown in the Fig. 9.
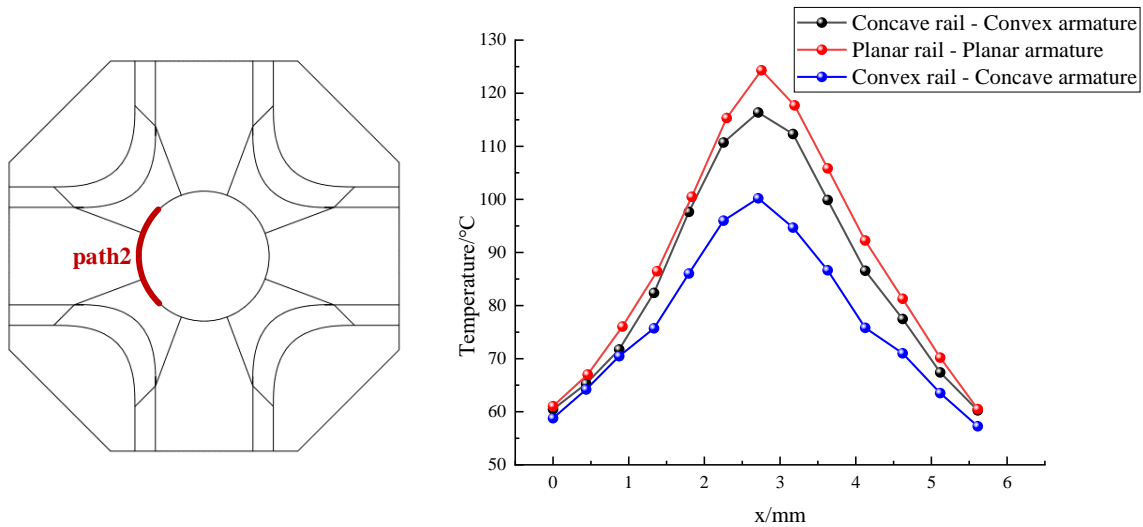
FIGURE 9. Schematic diagram of path 2 and temperature distribution

As shown in the Fig. 9, the temperature on the edge path of the electromagnetic shield hole shows a symmetrical pattern, the highest temperature on the path of the concave rail-convex armature structure is 116.37°C, the highest temperature of the planar rail-plane armature structure is 124.32°C, and the highest temperature of the convex rail-concave armature structure is 100.2°C. The temperature of the convex rail-concave armature structure on the path is smaller than the other two structures, from the perspective of temperature field, the convex rail-concave armature structure can protect the munition better than the other two structures to avoid the risk of failure or premature detonation of the loaded munition due to high temperature [15].

B. Joule heat analysis of different configurations of rail.

During the operation of the electromagnetic launcher, the armature is generally used once, while the rail needs to be used for a long time, therefore, it is necessary to analyze the Joule heat of the rail of the four-rail electromagnetic launcher of three configurations. According to the simulation results, it is known that the temperature peaks of the rails with concave rail-convex armature, planar rail-planar armature, and convex rail-concave armature are 107.34°C, 89.42°C, and 84.86°C, respectively, during operation. In order to better observe the temperature distribution on the rail, the rail tail and the contact surface of the armature rail are taken as the study objects respectively, and the Joule heat is analyzed and studied.

Fig. 10 shows a cross-sectional view of the temperature distribution due to Joule heat at the tail of the four-rail electromagnetic launcher orbit for the three structures, with units in degrees Celsius (°C).
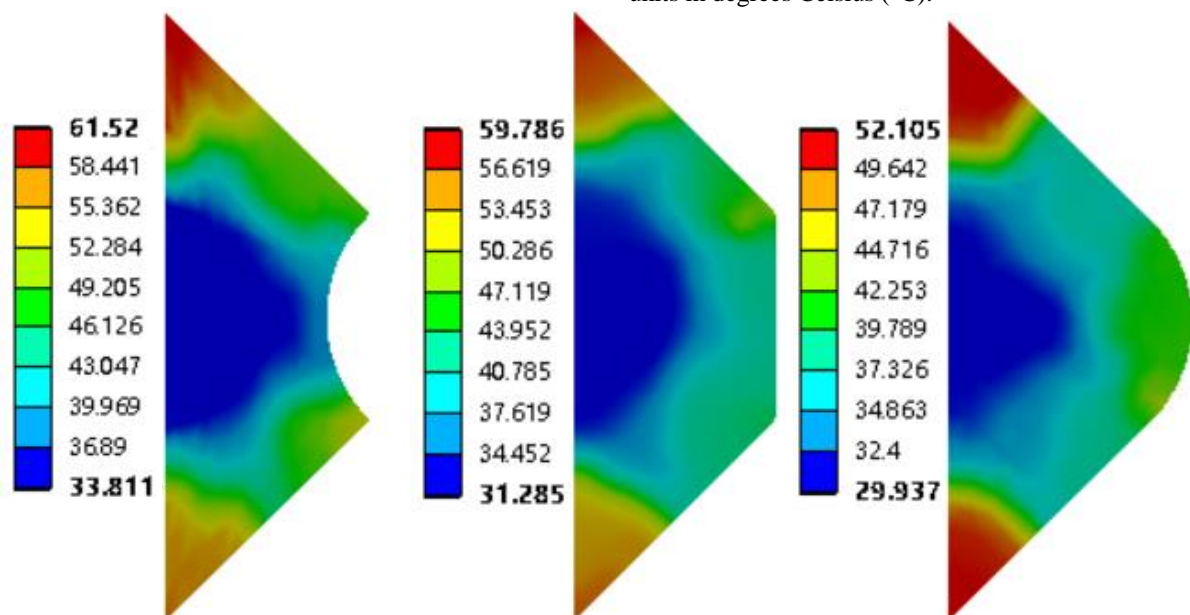

FIGURE 10. Cross-sectional view of temperature distribution at the end of the rail for different configurations
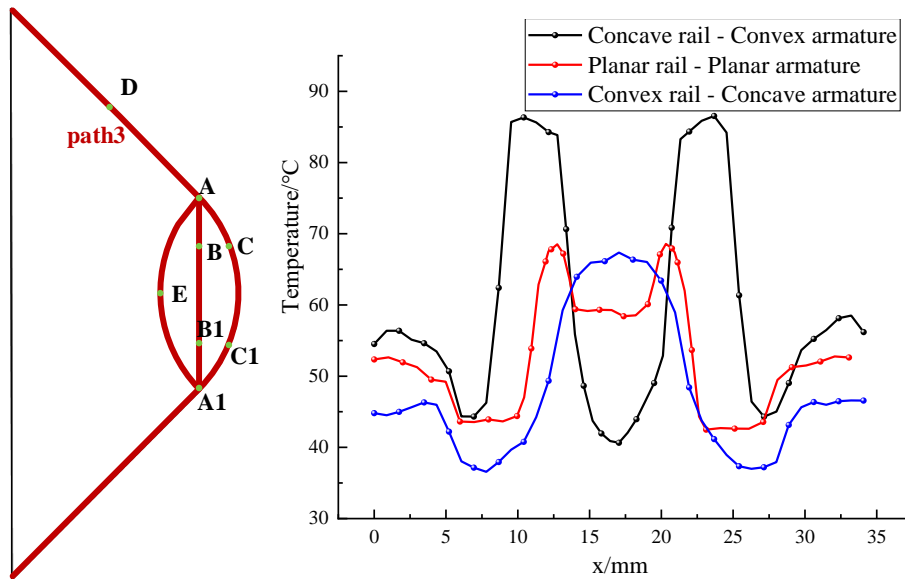
FIGURE 11. Schematic diagram of path 3 and temperature distribution

From the above cross-sectional diagrams, it can be learned that the maximum temperatures at the trailing part of the rails of three configurations of electromagnetic launchers, namely, concave-rail-convex armature, planar-rail-plane armature and convex-rail-concave armature, are 61.52°C, 59.79°C and 52.11°C, respectively. The Joule heat on the orbits of the three configurations is mainly concentrated at the edge of the orbit, which is caused by the skinning effect and proximity effect of the current. The Joule heat on the contact surface of the pivot rail is more concentrated at the sides for the concave and planar rails, while it is more concentrated at the center of the contact surface of the pivot rail for the convex rail [16].

In the contact part of the end section of the rail and armature arm where the Joule heat concentration problem is more obvious, take the transverse path shown in Fig. 11 and get the temperature distribution on the path as shown in Fig. 11.

As shown in the Fig. 11, the temperature distribution of the electromagnetic launcher for all three configurations shows an axisymmetric pattern along the path. Similar to the tail of the rail, all three configurations show different degrees of temperature concentration at the edge of the rail, which is the result of the current proximity effect and skin effect. The peak temperature of the concave rail appears near the point A where the contact between the rail and the armature begins, and the lowest temperature appears at the point E on the contact surface of the pivot rail, because the raised structure of the concave rail at the point A is more likely to lead to the concentration of current, which makes the current on the contact surface of the pivot rail flow more from the point A to the armature [17]. The peak temperature of the planar rail appears at section AB, while the temperature is lower at the middle part of the pivot rail contact surface, section BB1. The peak temperature of the

convex rail is found in the middle of the contact surface of the pivot rail, CC1, and the temperature decreases from the center of the pivot rail contact to the edge of the rail until the point D where the skin effect and the proximity effect affect the current, where the temperature increases again. Among the three configurations, the convex rail has the lowest peak temperature and the temperature at the rail edge decreases compared with the other two configurations, indicating that the convex rail-concave armature configuration improves the current concentration problem caused by the current skin effect and proximity effect, which is also consistent with the conclusion of the literature [10], so the convex rail-concave armature structure is more advantageous in terms of temperature field.

C. Influence of armature structure parameters on Joule heat

According to what was discussed in the previous section, Joule heat is mainly concentrated in the throat position area on the armature, so it is necessary to study the influence of armature throat parameters on Joule heat, and the armature throat area, where Joule heat concentration is a serious problem, is selected as the research object to analyze the influence of armature throat structure parameters on Joule heat of electromagnetic launcher. Table III shows the maximum temperature during operation of the four-rail electromagnetic launcher with different throat radii [18-19].

TABLE III. Maximum temperature during operation of four-rail electromagnetic launchers with different throat radii

Armature throat radius r (mm)	Maximum temperature (°C)
2	277.72
2.25	263.96
2.5	252.55
2.75	224.35
3	213.39

According to the data in the Table III, it is known that the larger the radius of the throat, the lower the maximum temperature during the operation of the four-rail electromagnetic launcher, indicating that the increase of the radius of the throat can mitigate the current concentration problem and provide a feasible solution to alleviate the Joule heat concentration problem.

V. Conclusion

In this paper, by analyzing the Joule heat generation mechanism of the four-rail electromagnetic launcher, establishing a mathematical model for Joule heat calculation, and simulating the temperature field of the four-rail electromagnetic launcher with three armature structures, the following conclusions were drawn.

(1) Among the three structures, the average temperature rise rate of the four-rail electromagnetic launcher with convex rail-concave armature structure is the lowest, at $40.38℃/ms$, which is 25.87% lower than that of the planar rail-plane armature structure, and 18.26% lower than that of the concave rail-convex armature structure.

(2) The Joule heat of the electromagnetic launcher of the three structures has a serious problem of concentration at the throat position of the armature, and the temperature of the convex rail-concave armature structure is smaller than that of the other two structures at all places on the throat path; due to the proximity effect and skin effect of the current, the Joule heat of the rail is concentrated at the edge of the rail and on the contact surface of the armature rail.

(3) Considering the safety of armature-carrying ammunition and the temperature rise of the rail, the convex rail-concave armature structure has better performance and is more conducive to prolonging the service life of the electromagnetic rail launcher.

(4) With the increase of the throat radius, the peak Joule heat temperature of the four-rail electromagnetic launcher with the convex-rail-concave armature structure decreases, and the Joule heat concentration problem is effectively alleviated.

REFERENCES

[1] J. Y. Lu, J. H. Feng, K. Li et al., "Review of research on ultra-high-speed guided projectiles," Journal of Harbin Engineering University, 2021, {4} (10):1-12. DOI:10.11990/jheu.202008006.

[2] Y. Wang, "On electromagnetic launcher to open the era of electromagnetic weapons," Electrical Technology, 2010, (S1): 1-4. DOI: CNKI: SUN: DQJS.0.2010-S1-003.

[3] W. M. Ma, J. Y. LU, X. P. LI, "Electromagnetically launched hypervelocity integrated projectile," Journal of the National University of Defense Technology,2019,41(4):1-10.1. DOI:10.11887/j.cn.201904001.

[4] T. D. Li, G. Feng, S. W. Liu et al., "Influence of four-rail electromagnetic launcher rail configuration on current distribution[J]. Weapon Materials Science and Engineering," 2021,44(05):5-11. DOI: 10.14024/j.cnki.1004-244x.20210601.001.

[5] T. D. Li, G. Feng, S. W. Liu et al., "Static analysis of pivot rails with different configurations of four-rail electromagnetic launcher [J].

[6] Journal of Ballistics,"2021,33(01):90-96. DOI: 10.12115/j.issn.1004-499X(2021)01-014.

[6] J. P. BARBER, A. CHALLITA, MAAS B et al., "Contact transition in metal armatures," IEEE Transactions on Magnetics, 1991, 27(1):228-232. DOI: 10.1109/20.101031.

[7] BARBER J P, THURMOND L E I, "Contact current carrying limits," Proceedings of the Thirty Fifth Meeting of the IEEE Holm Conference on Electrical Contacts. Chicago: IEEE, 1989. DOI: 10.1109/HOLM.1989.77915.

[8] D. Motes, J. Keena, K. Womack et al., "Thermal analysis of high-energy railgun tests," IEEE Transactions on Plasma Science, 2011, 40(1): 124-130. DOI: 10.1109/TPS.2011.2174375.

[9] L. K. Zhao, Z. G. Tian, L. Y. Jin, "Temperature field and Non-Fourier heat effect of launching electromagnetic rail," Journal of Ordnance Equipment Engineering, 2020, 41(03): 57-61+66. DOI: 10.11809/bqzbgcxb2020.03.011.

[10] X. J. Li, M. Wan, Z. H. Wang et al. "Numerical simulation of rail temperature field and thermal stress of electromagnetic railgun," Fire and command and control, 2017, 42(02): 154-158. DOI: 10.3969/j.issn.1002-0640.2017.02.033.

[11] F. Gong, W. Wei, H. H. Guo. "Analysis of electrothermal properties of commonly used materials for electromagnetic rail guns," Journal of Ballistics, 2018, 30(03): 78-81+87. DOI: 10.12115/j.issn.1004-499X(2018)03-014.

[12] Holm, Ragnar. Electric Contacts Handbook /-3rd ed[M]. Springer-Verlag, 1958, pp,10-18.

[13] A. B. Nong, S. Ma, F. Yang et al. "Analytical method for solving the heat production in the orbit of electromagnetic gun firing process," Weapon Materials Science and Engineering,2022,45(02):17-25. DOI: 10.14024/j.cnki.1004-244x.20220101.001.

[14] Z. G. Tian, X. Y. An, Y. Yang et al. Analysis of temperature field of composite rail under launching state of railgun [J]. Journal of Yanshan University, 2019, 43(03): 271-277. DOI: 10.3969/j.issn.1007-791X.2019.03.011.

[15] Li Shuai, "Study of electromagnetic characteristics and temperature field effects of electromagnetic rail gun caliber," M.S. thesis, Yanshan University,2020. DOI: 10.27440/d.cnki.gysdu.2020.000245

[16] H. Zhang, S. Li, X. Gao et al., "Distribution Characteristics of Electromagnetic Field and Temperature Field of Different Caliber Electromagnetic Railguns," IEEE Transactions on Plasma Science, 2020, 48(12): 4342-4349. DOI: 10.1109/TPS.2020.3034121.

[17] W. Huang, L. M. Yang, G. N. Shi et al., "Damage Behavior of CuCrZr Alloy Rail during Electromagnetic Launching," Journal of ordnance industry, 2020,41(05): 858-864. DOI: 10.3969/j.issn.1000-1093.2020.05.004.

[18] S. F. Gao, H. Y. Li, B. M. Li, "Multi-field coupled finite element simulation of round bore multi-rail electromagnetic gun barrel," Journal of Ordnance Equipment Engineering, 2019, 40(02): 54-58+124. DOI: 10.11809/bqzbgcxb2019.02.011.

[19] Tang B, Lin Q, Li B. "An optimization method for passive muzzle arc control devices in augmented railguns," Defence Technology, 2022, 18(2): 271-279. Doi: org/10.1016/j.dt.2021.01.001.